Phytomedicine 17 (2010) 714–720

Contents lists available at ScienceDirect

Phytomedicine

journal homepage: www.elsevier.de/phymed

Thymoquinone, a potential therapeutic agent of *Nigella sativa*, binds to site I of human serum albumin

G. Lupidi [a,1], A. Scire [b,1], E. Camaioni [c], K.H. Khalife [a], G. De Sanctis [a], F. Tanfani [b], E. Damiani [b,*]

[a] *Dipartimento di Biologia M.C.A., Università degli Studi di Camerino, Camerino, Italy*
[b] *Dipartimento di Biochimica, Biologia e Genetica, Università Politecnica delle Marche, Ancona, Italy*
[c] *Dipartimento di Chimica e Tecnologia del Farmaco, Università degli Studi di Perugia, Perugia, Italy*

ARTICLE INFO

Keywords:
Thymoquinone
Nigella sativa
Human serum albumin
Drug-protein complex
FT-IR
Fluorescence quenching
Circular dichroism
Molecular docking

ABSTRACT

Thymoquinone (TQ) is the main constituent of *Nigella sativa* essential oil which shows promising *in vitro* and *in vivo* antineoplastic growth inhibition against various tumor cell lines. Because of the increasing interest to test it in pre-clinical and clinical researches for assessing its health benefits, we here evaluate the interactions between TQ and human serum albumin (HSA), a possible carrier of this drug *in vivo*. Binding to HSA was studied using different spectroscopic techniques. Fourier transform infrared (FT-IR) and circular dichroism (CD) spectroscopies suggest that the association between TQ and HSA does not affect the secondary structure of HSA. Using fluorescence spectroscopy, one mole of TQ was found to bind one mole of HSA with a binding constant of $2.39 \pm 0.2\ 10^4\ M^{-1}$. At 25 °C (pH 7.4), van't Hoff's enthalpy and entropy that accompany the binding were found to be $-10.24\ kJ/mol^{-1}$ and $45\ J/mol^{-1}K^{-1}$ respectively. The thermodynamic analysis of the TQ-HSA complex formation shows that the binding process is enthalpy driven and spontaneous, and that hydrophobic interactions are the predominant intermolecular forces stabilizing the complex. Furthermore, displacement experiments using warfarin and ibuprofen indicate that TQ could bind to site I of HSA, which is also in agreement with the results of the molecular modeling study.

Introduction

Thymoquinone (TQ) is the main constituent of *Nigella sativa*, whose seeds and essential oil have been traditionally employed in folk medicine and is now recognized as a herbal remedy of a number of pharmacopoeia (Gali-Muhtasib et al. 2006; Padhye et al. 2008). Pharmacological studies have demonstrated that TQ possesses important properties such as: analgesic and anti-inflammatory (El Gazzar et al. 2006; Padhye et al. 2008), protection of organs against oxidative damage induced by a variety of free radical generating agents (including carbon tetrachloride, cis-platin, doxorubicin and recently HIV-1 protease inhibitor) (El Gazzar et al. 2006; Gali-Muhtasib et al. 2006; Padhye et al. 2008; Chandra et al. 2009), inhibition of eicosanoid generation) and membrane lipid peroxidation (Hosseinzadeh et al. 2007). Amongst the various bioactivities examined for TQ, many investigators have shown that the growth inhibitory effects of TQ are specific to cancer cells: significant anti-neoplastic activity was observed against human pancreatic, adenocarcinoma, uterine sarcoma and leukemic cell lines, while it is minimally toxic to normal cells (Gali-Muhtasib et al. 2004a, 2004b, 2006; Padhye et al. 2008; Edris 2009). Additionally, it has been reported that TQ and *Nigella sativa* could also be potent chemopreventive agents (Khan and Sultana 2005). There is now evidence to support the idea that the reduced form of TQ (DHTQ or derivatives) acts as an effective antioxidant in cellular systems by scavenging oxygen radicals. DHTQ performs this function through the redox transition of the benzoquinone ring. Enzymatic and nonenzymatic systems could transform TQ to DHTQ thus maintaining TQ in its reduced form. In a recent study (Khalife and Lupidi 2007), we showed that under physiological conditions TQ reacts with GSH or NADH and NADPH through a spontaneous reaction to produce species (DHTQ-GS or DHTQ) whose antioxidant properties were higher than those of TQ and similar to those of Trolox, a water soluble analogue of vitamin E. The high potency and low systemic toxicity of TQ make it a promising alternative to conventional therapeutic drugs. Thymoquinone is a promising compound with

Abbreviations: TQ, thymoquinone; DHTQ, dihydrothymoquinone; DHTQ-GS, glutathionyl-dihydrothymoquinone; HSA, Human serum albumin; CD, Circular Dichroism; FT-IR, Fourier transform infrared; GSH, glutathione; NADH, nicotinamide adenine dinucleotide reduced form; NADPH, nicotinamide adenine dinucleotide phosphate reduced form.

* Corresponding author. Tel.: +39 712204135; fax: +39 712204398.
E-mail address: e.damiani@univpm.it (E. Damiani).
[1] These authors contributed equally to the work.

0944-7113/$ - see front matter © 2010 Elsevier GmbH. All rights reserved.
doi:10.1016/j.phymed.2010.01.011

significant *in vitro* and *in vivo* antitumor activities against different tumor models (Ivankovic et al. 2006). No data on TQ plasma concentrations can be found at present in the literature, but some authors report the use of different ranges of TQ and *Nigella sativa* oil in several important diseases. On the other hand, the use of high doses of TQ (50 and 100 mg/kg) indicate that both *Nigella sativa* oil and TQ are protective against gastric lesions which may be related to the conservation of the gastric mucosal redox state (El-Abhar et al. 2003). Recently, TQ has been reported to be a potent antitumor agent against human colorectal cancer cells. The use of TQ (40 μM) injected intraperitoneally (i.p.) significantly decreased cell invasion and suppressed tumor growth in different mice colon cancer models (Gali-Muhtasib et al. 2008; Yi et al. 2008). In this context, the question of possible target molecules, its mode of interaction with the target and bioavailability are important issues of current pharmacological research concerning TQ. In particular, the interaction of a drug with blood components has great influence on its bioavailability, distribution in the body, metabolism and excretion. Plasma proteins serve as transport carriers for drugs and the study of their binding properties is an important field in drug research. Human serum albumin (HSA) is the most abundant protein in blood plasma and plays an important role in the regulation of plasmatic concentrations of several drugs, including endogens and exogens. A study of drug action at the molecular level is necessary to obtain information on the potential mechanism of the drug–protein interaction, and HSA is usually used as a model protein for elucidating drug–protein complexes. The affinity of a drug to a protein would directly influence the concentration of the drug in the binding site and duration of the effectual drug, and consequently contribute to the magnitude of its biological actions *in vivo*. In this work, the binding of HSA with TQ was characterized using fluorescence spectroscopy whereas a possible effect on the protein's secondary structures induced by TQ were studied by circular dichroism (CD) and Fourier transform infrared (FT-IR) spectroscopies. Based on the results obtained, a molecular docking study was used to characterize the predominant intermolecular forces stabilizing the complex of TQ with the binding site on HSA.

Materials and methods

Materials

Lyophilized human serum albumin (HSA), HEPES, Menadione, Warfarin and Ibuprofen were purchased from Sigma Chemical Company. HSA was used without further purification and its molecular weight was assumed to be 66,500. Thymoquinone, deuterium oxide (99.9 % ^2H_2O) deuterated ethanol (Et-O^{2}H) and NaO^{2}H were purchased from Aldrich. All other reagents were of analytical grade and doubly distilled water was used throughout all the experiments.

Preparation of samples for FT-IR measurements

Human serum albumin was analyzed in 50 mM Hepes/NaOH pH 7.4, in the absence or in the presence of 2.4 mM thymoquinone. The p^{2}H value corresponds to the pH meter reading +0.4 (Salomaa et al. 1964). Typically, about 1.8 mg of HSA were dissolved in 200 μl of buffer and concentrated to a volume of approximately 50 μl using a "30 K Centricon" micro concentrator (Amicon) at 3000 g and 4 °C. Subsequently, 200 μl of buffer were added and the protein solution was concentrated again. This procedure was repeated three times to hydrate the protein completely with the 50 mM Hepes/NaO^{2}H p^{2}H 7.4 buffer. In the last washing, the protein solution was concentrated to 45 μl, obtaining a 4% (w/v) final protein concentration used for infrared measurements. For the experiments performed in the presence of TQ, a proper amount (0.9 μl) of TQ/Et-O^{2}H solution (120 mM) was added to the concentrated protein solution (45 μl), obtaining a TQ/protein molar ratio equal to 4.

FT-IR measurements

The concentrated protein sample was placed in a thermostated Graseby Specac 20500 cell (Graseby-Specac Ltd, Orpington, Kent, UK) fitted with CaF_2 windows and a 25 μm Teflon spacer. FT-IR spectra were recorded by means of a Perkin-Elmer 1760-x Fourier transform infrared spectrometer using a deuterated triglycine sulphate detector and a normal Beer-Norton apodization function. At least 24 hours prior to and during data acquisition, the spectrometer was continuously purged with dry air at a dew point of −70 °C. Spectra of buffers and samples were acquired at 2 cm^{-1} resolution under the same scanning and temperature conditions. In the thermal denaturation experiments, the temperature was raised in 5 °C steps from 20 °C to 95 °C using an external bath circulator (HAAKE F3). The actual temperature in the cell was controlled by a thermocouple placed directly onto the windows. Before spectrum acquisition, samples were maintained at the desired temperature for the time necessary for the stabilization of temperature inside the cell (6 min). Spectra were processed using the SPECTRUM software from Perkin-Elmer. Correct subtraction of ^2H_2O was judged to yield an approximately flat baseline after the removal of the ^2H_2O bending absorption close to 1220 cm^{-1} (Tanfani et al. 1997). The deconvoluted parameters were set with a gamma value of 2.5 and a smoothing length of 60. Second derivative spectra were calculated over a 9-data-point range (9 cm^{-1}). The temperature of protein melting (T_m) was obtained as previously described (Meersman et al. 2002).

Circular dichroism measurements

Circular dichroism (CD) experiments were performed on a Jasco J710 spectropolarimeter in the far UV region (190 – 250 nm). Cell length was 0.1 cm, the buffer was 20 mM potassium phosphate pH 7.4 and the temperature was 20 °C. The concentration of HSA was 1 μM while that of TQ was 0.5, or 1, or 10 μM. All spectra reported are the average of eight measurements and were corrected by baseline subtraction.

Fluorescence quenching studies

Fluorescence spectra related to the titration of HSA with TQ were measured on an ISS GREG-200 spectrofluorimeter at 20 °C. Quenching experiments were performed on 2 ml of HSA (15.5 μM) in 50 mM phosphate buffer pH 7.4. The solution was titrated by sequential additions of concentrated stock ethanolic solutions of TQ or menadione so that the volume increment was negligible as was the concentration of alcohol in the mixture (less than 1%). All samples were measured after five minutes at four different temperatures. The fluorescence intensity measured for the different compounds tested were corrected for dilution and for their absorption at excitation and emission wavelengths (Lakowicz 1999) using the relationship (Eq. (1)):

$$F_{cor} = F_{obs} x e^{(Aex + Aem)/2} \quad (1)$$

where F_{cor} and F_{obs} are the fluorescence intensity corrected and observed, respectively; A_{ex} and A_{em} are the absorbance of systems at excitation and emission wavelengths, respectively.

For fluorescence quenching experiments, Stern-Volmer's equation was used (Eq. (2)):

$$F_0/F = 1 + k_Q \tau_0 [D] = 1 + K_{sv}[D] \quad (2)$$

where F_0 and F represent the fluorescence intensity in the absence and in the presence of drug. [D] is the concentration of drug and K_{sv} is the Stern-Volmer constant which is equal to k_Q x τ_0, where k_Q is the bimolecular quenching rate constant and τ_0 is the average fluorescence lifetime of the fluorophore in the absence of drug.

In the case of fluorescence caused only by the protein and assuming that the TQ-HSA complex (1:1 stoichiometry) is responsible for the fluorescence quenching of the protein, the observed change in fluorescence of HSA after binding with increasing concentrations of TQ, can be related to the following relationship:

$$\log(F_0 - F)/F = n \log K_A - n \log 1/([D_t] - [P_t](F_0 - F)/F_0)) \quad (3)$$

where any assumed conditions concerning free protein or free/bound drug concentrations are not required (for complete derivation of Eq. (3) see references (Timaseff 1972; Ross and Subramanian 1981; He and Carter 1992)).

Displacement experiments were performed for identifying the putative binding site of TQ using marker ligands displacement: Warfarin, specific for site I and Ibuprofen, specific for site II. These were performed on 2 ml of HSA (15.5 μM) in 50 mM phosphate buffer pH 7.4, in the presence or absence of Warfarin (7.5 μM) or Ibuprofen (7.5 μM). The solutions were titrated by sequential additions of concentrated stock ethanolic solutions of TQ and analysis of binding data were assessed using Eq. (3).

Thermodynamic parameters

The thermodynamic parameters of the binding reaction are the main evidence for confirming the binding mode. For this purpose, the temperature dependence of the binding constants was measured for different temperatures at which HSA did not undergo any structural degradation. The thermodynamic parameters were analysed using van't Hoff's equation:

$$\ln K_A = -\Delta H^0/RT + \Delta S^0/R \quad (4)$$

where K_A is the binding constant at the corresponding temperature, R is the gas constant, T is the absolute temperature. The free energy change is estimated from the following relationship:

$$\Delta G^0 = -RT \ln K_A. \quad (5)$$

Finally the entropy change (ΔS^0) is obtained by using the parameters calculated:

$$\Delta G^0 = \Delta H^0 - T\Delta S^0 \quad (6)$$

Molecular modelling/docking studies

All molecular modelling calculations were performed using the following software packages: ACD/Labs 10 Freeware (Advanced Chemistry Development Inc., Ontario, Canada) and VegaZZ 2.0.8 (Pedretti et al. 2002) for ligand preparation on Windows XP operating system; AutoDock 3.0.5 (Goodsell et al. 1996) and AutoDockTools 1.4.4 (Sanner 1999) for docking, visualization and rendering simulations on Ubuntu 8.10 Linux operating system running on Pentium IV 2.0 GHz Personal Computer. In particular the structure of TQ was constructed using Chemsketch (ACD/Labs), 3D optimized and exported as mol file. The geometry optimization of TQ was refined with the VegaZZ batch processing MOPAC script (mopac.r; keywords: MMOK, PRECISE, GEO-OK) using AM1 semiempirical theory (Dewar et al. 1985) and then converted and stored as mol2 file. Details on the docking methodology used by Autodock 3.05 are fully described elsewhere (Goodsell et al. 1996). In this study, using AutoDockTools (an application to setup, launch and analyze AutoDock) both the ligand TQ and the HSA protein were prepared for docking studies. X-ray crystal structure of HSA (pdb code 1BM0, res. 2.5 Å) was retrieved from Brookhaven Protein Database (Berman et al. 2000). Water molecules were removed and the atomic coordinates of chain A of 1BM0 were stored in a separate file and used as input for AutoDockTools. Thus, polar hydrogens, Kollman charges and solvatation parameters were added. In case of the ligand TQ imported as mol2 file, non-polar hydrogens were merged, and rotable bonds were defined. Lamarckian genetic algorithm with local search (GA-LS) was used as search engine, with a total of 100 runs for each binding site. In each run, a population of 150 individuals with 27000 generations and 250000 energy evaluations were employed. Operator weights for crossover, mutation and elitism were set to 0.8, 0,02 and 1, respectively. The two binding sites (subdomains IIA and IIIA, respectively) were defined using two grids of 70x70x70 points each with a grid space of 0.375 Å centred at coordinates x=35.26 y=32.41 z=36.46 for subsite IIA and x=14.42 y=23.55 z=23.31 for subsite IIIA, respectively. For local search default parameters were used. Cluster analysis was performed on the docked results using an RMS tolerance of 1.0 Å.

Results and discussion

Secondary structure and thermostability

CD and IR spectral data indicate no significant changes in secondary structure induced by TQ binding (Fig. 1). In particular, CD spectra reported in Fig. 1A show that addition up to 10 μM of TQ to HSA leads only to a tiny decrease in negative ellipticity without any changes in the spectrum shape, peak wavelength and the 222/208 nm peaks ratio, resulting in no rearrangements in secondary structure.

The absorbance and resolution-enhanced FT-IR spectra of HSA (continuous line) and HSA-TQ (dashed line) at 20 °C are shown in Fig. 1B. The amide I' band (1700 - 1600 cm^{-1} range) contains the information on protein secondary structure (Arrondo et al. 1993). In the amide I' region, the deconvoluted and second derivative spectra of HSA and HSA-TQ show three bands that are due to α-helices (1651.9 cm^{-1}, 1632.1 cm^{-1}) and turns/bends (1678.2 cm^{-1}) (Arrondo et al. 1993; Okuno et al. 2006). The bands below 1620 cm^{-1} are due to amino acid side chain absorption (Barth and Zscherp 2002). Since spectra of HSA and of HSA-TQ are superimposable, we can state that the binding of TQ does not alter the secondary structure of HSA.

The thermal denaturation curves for HSA and HSA-TQ (Fig. 1C) were obtained by monitoring the α-helix band intensity (1651.9 cm^{-1}) versus temperature. The figure shows that HSA-TQ is more thermostable than HSA being the Tm equal to 65.4 °C and 61.9 °C, respectively.

Fluorescence quenching and binding analysis

Fluorescence quenching of the single tryptophan residue in HSA was used to measure the drug-binding affinity. The addition of TQ to HSA solution caused a decrease in intrinsic fluorescence emission spectra of the protein upon excitation at 290 nm (Fig. 2). The fluorescence intensity of the protein decreases in the presence of increasing concentrations of TQ and a small blue

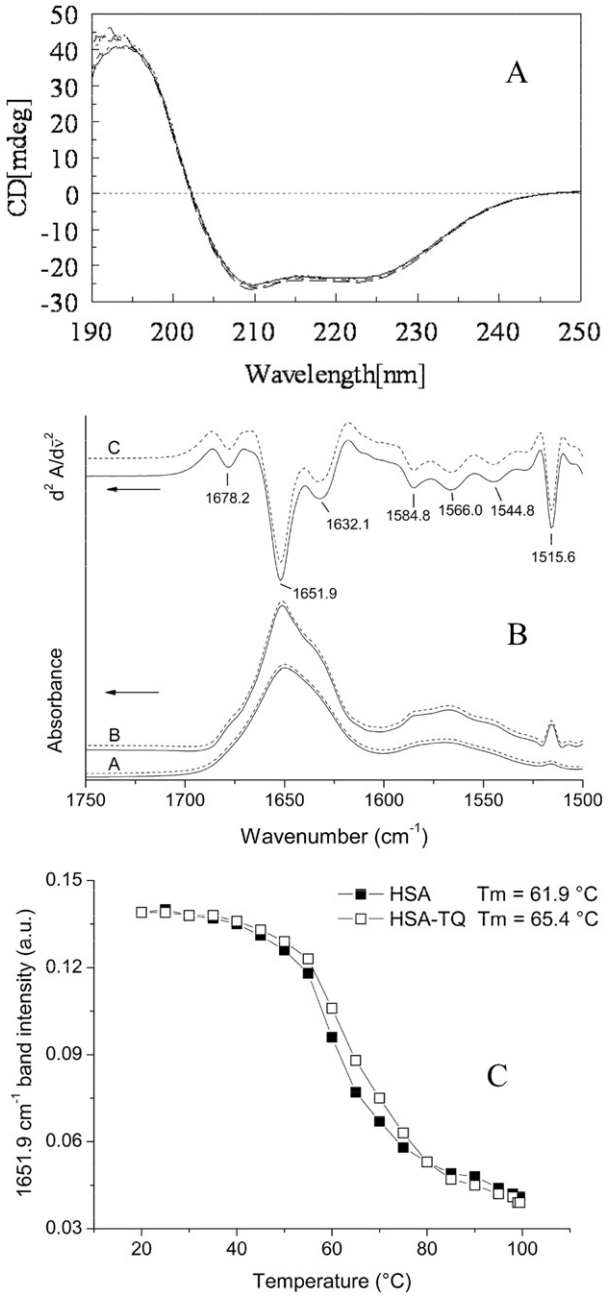

Fig. 1. Secondary structure and thermostability data. **1A**: Circular dichroism spectra of HSA with TQ. Long dashed line, 1 μM HSA; dash-dotted line, 1 μM HSA in the presence of 0.5 μM TQ; continuous line, 1.0 μM HSA in the presence of 1.0 μM TQ; dotted line, 1.0 μM HSA in the presence of 10 μM TQ. **1B**: Absorbance (A), deconvoluted (B) and second derivative (C) FT-IR spectra of HSA (continuous line) and HSA-TQ (dashed line). **1C**: Thermal denaturation plots of HSA and HSA-TQ: the graph was obtained by monitoring the intensity of the 1651.9 cm^{-1} band (α-helix) in the absorbance spectra as a function of temperature. Closed and open squares refer to HSA and HSA-TQ, respectively. T_m was calculated as described in materials and methods.

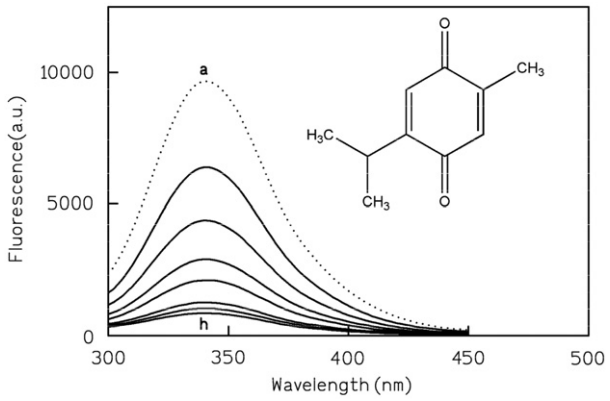

Fig. 2. Fluorescence spectra of the complex TQ-HSA. Assay conditions: 50 mM potassium phosphate buffer pH 7.4, 15.5 μM HSA and increasing concentrations of TQ from 0 to 119.6 μM from (a) to (i). Inset: structure of thymoquinone.

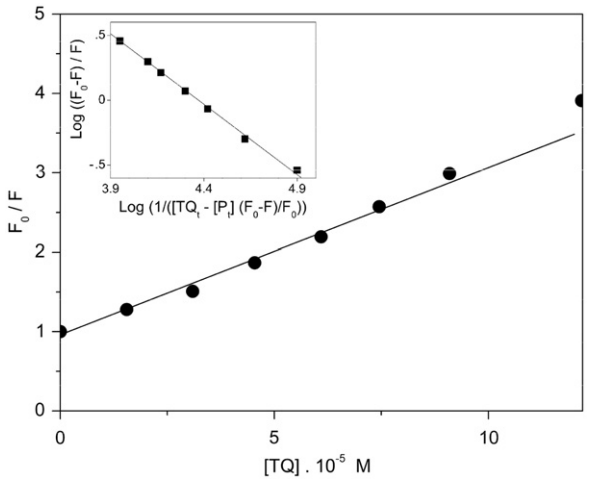

Fig. 3. Stern-Volmer plot for HSA fluorescence quenching by TQ. Assay conditions as reported in Fig. 2. Inset, Plot of log(F_0-F)/F vs log(1/([TQ_t] – [P_t](F_0-F)/F_0)) for the binding of TQ to HSA.

shift was observed for the maximum emission wavelength of HSA that indicates binding of TQ to HSA.

The Stern–Volmer quenching constant was calculated from the linear range (C_{drug}/C_{HSA} from 0.1 to about 5) (Fig. 3), giving a value of $K_{sv} = (2.33 \pm 0.07) \times 10^4\ M^{-1}$ (R=0.99, n=8) calculated according to Eq. (2). Using an average fluorescence lifetime of about 5 ns calculated from different values of fluorescence lifetime for HSA previously reported (Gelamo et al. 2002; Mishra et al. 2005; Xie et al. 2006; Bogdan et al. 2008), the bimolecular quenching rate constant was obtained from the value of K_{sv}, $k_Q = 4.66 \pm (0.14) \times 10^{12}\ M^{-1}\ s^{-1}$. The derived value for k_Q is two orders of magnitude greater than the maximum diffusion quenching rate constant (K_{dif}) of the biomolecule ($K_{dif} = 2.0 \times 10^{10}\ M^{-1}\ s^{-1}$) (Mishra et al. 2005; Bogdan et al. 2008). This therefore indicates that the fluorescence quenching process of HSA was caused by a specific interaction between HSA and TQ and may be governed by a static quenching complex formation (Bogdan et al. 2008). For the static quenching process, Eq. (3) was applied since this had been previously used for determining the binding constants for the association of different flavonoids to HSA (Bi et al. 2005). From the plot of log(F_0-F/F) versus log(1/([Dt]-(F_0-F)[Pt]/F_0)) the number of binding sites, n=1.11 and the binding constant, $K_A = 2.39\ (\pm 0.2) \times 10^4\ M^{-1}$ for the association of TQ to HSA can be obtained (inset Fig. 3). The binding parameters for TQ-HSA interaction as well as for other compounds are summarized in Table 1. The data show that the value of K_A for TQ is similar to that of menadione (vitamin K, a natural quinone with structural features similar to TQ) and lower than that of other phenol derivatives, such as flavonoids reported in Table 1. These substances are common dietary components that have many potent biological properties and their proposed use as anticarcinogens and cardioprotective agents have prompted a dramatic increase in their consumption as dietary supplements. Association of these compounds with TQ treatment

could result in the availability of higher concentrations of the free drug in plasma, thus enhancing its pharmacological effects. Studies are in progress to evaluate these potential effects.

Analysis of binding of TQ to HSA was also carried out using tryptophan fluorescence quenching at 340 nm at various temperatures. TQ strongly binds to HSA and the association constant decreases with increasing temperature (Fig. 4). From the temperature dependence of the binding constant, it is possible to estimate the values for the thermodynamic functions involved in the binding process. From the ln K_A versus 1/T plot (inset Fig. 4), ΔH^0 and ΔS^0 for the binding process were determined. The values of ΔH^0, ΔS^0 and ΔG^0 are summarized in Table 2. The binding process was always spontaneous as demonstrated by the negative value of ΔG^0 and the formation of the TQ-HSA complex is an exothermic process, accompanied by negative enthalpy and positive entropy changes. Positive ΔH^0 and ΔS^0 values are frequently taken as typical evidence of hydrophobic interactions, while negative enthalpy and entropy changes arise from van der Waals and hydrogen bonding formation (Timaseff 1972; Ross and Subramanian 1981). Therefore from these results, the binding of TQ to HSA appears to involve hydrophobic interactions as shown by the positive value of ΔS^0 although a lower component of electrostatic interactions cannot be excluded. HSA has one tryptophan residue: Trp-214 is located within a hydrophobic pocket which is in a well-characterized binding cavity (subdomain IIA) for small aromatic molecules. The crystallographic analysis of HSA has also revealed that the major ligand binding sites are identified within this region (Carter and Ho 1994), hence one can hypothesize that the binding site for TQ to HSA could be mainly located in subdomain IIA.

Table 1
Fluorescence binding constants for the complex HSA-TQ, HSA-Menadione and other phenols.

	K_A (M^{-1})
Thymoquinone	$2.39 (\pm 0.2) \times 10^4$
Menadione	$3.28(\pm 0.3) \times 10^4$
Emodin (Sudlow et al., 1975)	3.18×10^5
Rhein (Sudlow et al., 1975)	2.20×10^5
Morin (Whitlam et al., 1979)	$1.13(\pm 0.14) \times 10^5$
Quercetin (Diana et al., 1989)	1.9×10^5

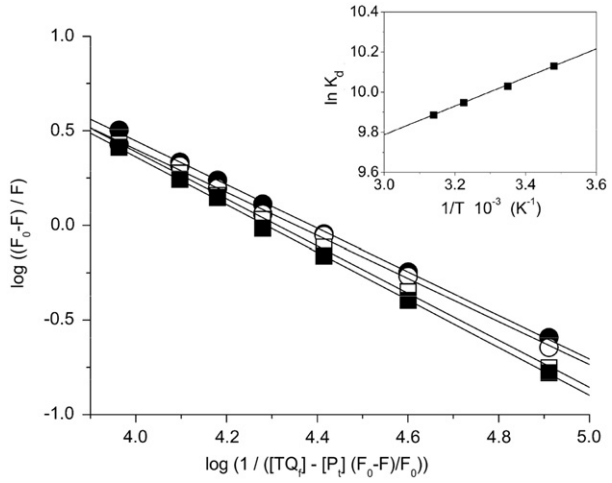

Fig. 4. Temperature dependence of TQ-HSA binding constant. Plot of log(F_0-F)/F vs log(1/([TQ_t] – [P_t](F_0-F)/F_0)) for the binding of TQ to HSA at (●) 288 °K; (○) 298 °K; (□) 310 °K; (■) 318 °K. Data were obtained with assay conditions as reported in Fig. 2. Inset: variation of ln K_A as function of 1/T for the binding of TQ to HSA.

Table 2
Thermodynamic parameters for the interaction HSA-TQ.

Temperature (°K)	ΔG^0(kJ/mol)	ΔH^0(kJ/mol)	ΔS^0(J/mol K)
288	−23.05	−10.24	45
298	−23.71		
310	−24.05		
318	−24.46		

The interaction of ligands with HSA occurs mainly in two regions. According to Sudlow's nomenclature (Sudlow et al. 1975), bulky heterocyclic anions bind to site I (located in subdomain IIA), whereas site II (located in subdomain IIIA) is preferred by aromatic carboxylates with an extended conformation. The IIIA subdomain is the most active in accommodating many ligands, for example, digitoxin, ibuprofen, tryptophan, aspirin show almost equal distributions between binding sites located in IIA and IIIA subdomains, while warfarin occupies a single site in subdomain IIA of site I. Ibuprofen, a nonsteroidal anti-inflammatory agent, and warfarin, an anticoagulant drug, are considered as stereotypical ligands for Sudlow's site II and Sudlow's site I, respectively (Diana et al. 1989; Loun and Hage 1994). Ibuprofen binds to Sudlow's site II with K_D=3.7 10^{-7} M, whereas warfarin binds to Sudlow's site I with K_D=3.0 x 10^{-6} M (Loun and Hage 1994). Indeed, subdomain IIA has recently been shown by X-ray crystallography to be one of the two principal sites on HSA for small hydrophobic ligands (He and Carter 1992). Hence, to provide further information on the binding site of TQ on HSA, displacement experiments were performed using warfarin and ibuprofen as specific displacement marker ligands for site I and site II, respectively. The results reported in Table 3 show that the binding constant of TQ on HSA decreased after addition of warfarin while the addition of ibuprofen did not significantly change the binding constant value. This indicates that warfarin (specific for site I) can displace TQ but ibuprofen (specific for site II) has no effect on binding of TQ to HSA. Overall, the displacement experiments imply that TQ interacts with HSA at site I in subdomain IIA. Previously it was reported that menadione (vitamin K3) interacts with bovine serum albumin (Shaikh et al. 2007), but no evidences have been reported on its binding site on the protein. The data reported in Table 3 indicate that in the presence of warfarin the binding constant of TQ to HSA is significantly lower and that in the presence of ibuprofen it is very similar to the control. Hence, the data suggest that menadione

Table 3
Fluorescence binding constants for the binding of TQ to HSA in the presence and in the absence of Warfarin and Ibuprofen.

	HSA K_A(M^{-1})	HSA-Warfarin K_A(M^{-1})	HSA-Ibuprofen K_A(M^{-1})
Thymoquinone	$2.39(\pm 0.2) \times 10^4$	$1.8(\pm .0.12) \times 10^4$	$2.2(\pm 0.11) \times 10^4$
Menadione	$3.28(\pm 0.3) \times 10^4$	$2.47(\pm 0.1) \times 10^4$	$3.01(\pm 0.12) \times 10^4$

binds to site I of HSA with a binding constant value similar to that reported for TQ.

Docking studies

With the aim to disclose the putative binding site of TQ in HSA and to confirm the results of the displacement experiments, a molecular modeling study was performed. The X-ray structure of HSA with high resolution (pdb code 1BM0, res. 2.5 Å) was used as a template to perform the docking experiments. The binding mode of TQ was predicted by using the Lamarckian genetic algorithm search engine implemented in AutoDock software package (Goodsell et al. 1996) for the two main drug binding sites I and II (Sudlow's nomenclature (Sudlow et al. 1975); subdomains IIA and IIIA of HSA, respectively). Thus, the two regions of interest used by AutoDock were defined in such a way to comprise the subdomains IIA and IIIA, respectively. The docking results are reported in Fig. 5. Indeed, after cluster analysis, using an RMSD-tolerance of 1.0 Å, of 100 docking runs for binding site I, 5 multi-member conformational clusters were found. The highest populated cluster contains 72 out of 100 conformations and resulted to be the lowest and hence the most energetically favorable cluster possessing an estimated docking energy of about -6.60 kcal/mol (Fig. 5A). Whereas for the binding site II, using the same approach, 12 distinct conformational clusters were found and the most populated (only 29 out of 100 conformations) was not the most energetically favorable cluster (-6.08 kcal/mol, Fig. 5B). Accordingly, one can argue that TQ shows a binding preference for the drug binding site I (subdomain IIA) of HSA. These results are in agreement with other experimental literature data. Indeed, it has been recently reported that quinone-related derivatives such as some naturally occurring anthraquinones bind to subdomain IIA of HSA or BSA (bovine serum albumin) (Bi et al. 2005; Li et al. 2007). The predicted binding model with the lowest

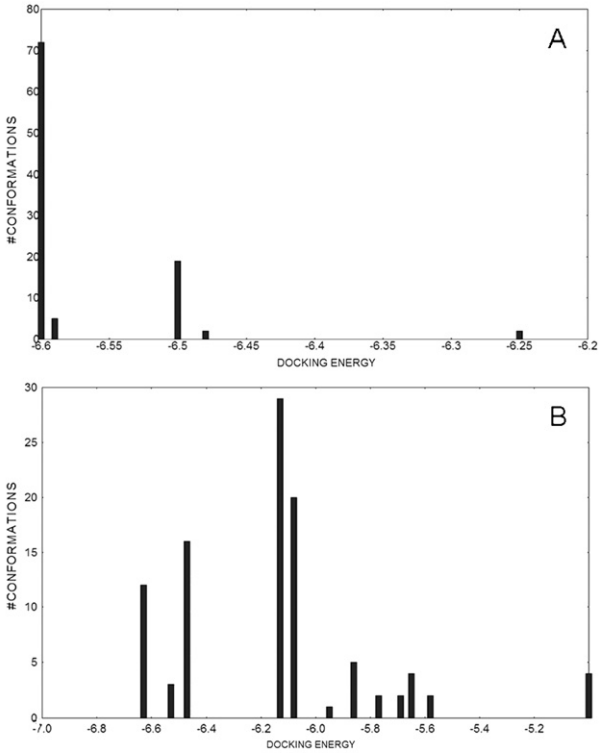

Fig. 5. Cluster analysis of the AutoDock docking runs of TQ in the drug binding site I (panel A) and II (panel B) subdomains IIA and IIIA of HSA, respectively.

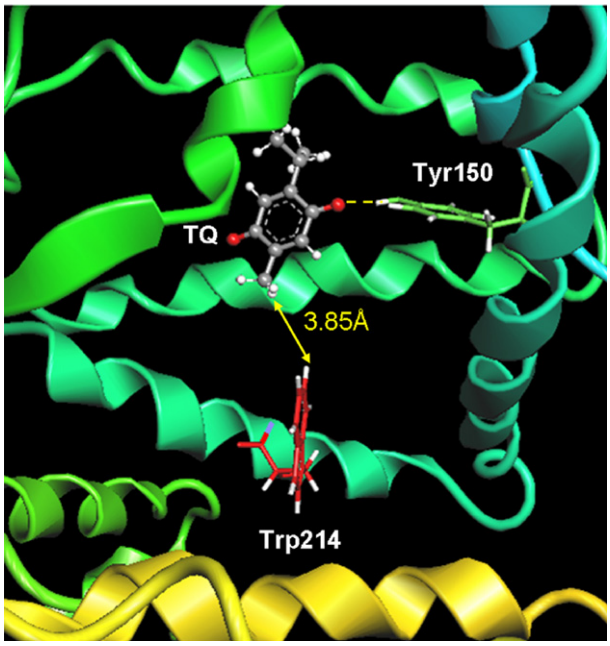

Fig. 6. Predicted binding orientation (lowest docking energy pose −6.60 Kcal/mol) of TQ (ball and stick rendered) in the subdomain IIA of HSA. Trp214 (red) and Tyr150 (green) are also displayed. (For interpretation of the references to color in this figure legend, the reader is referred to the web version of this article.)

docking energy was then used for further analysis. Indeed, as depicted in Fig. 6, TQ binds to subdomain IIA of HSA and is located at about 5 Å from the fluorescent Trp214, thus confirming the displacement experiments reported above. This TQ binding site is mostly included in a hydrophobic cleft walled by the following aminoacids: Tyr150, Leu199, Trp214, Leu219, Arg222, Leu238, Arg257, Leu260, Ala261, Ile264, Ser287, Ile290, and Ala291. The O-carbonylic in 2-position of TQ interacts with Tyr150 and Arg257 making two hydrogen bonds and the hindered isopropyl side chain is directed in a cleft formed by hydrophobic residues such as Leu260, Ala261, Ile290, and Ala291.

Conclusions

In conclusion, the results indicate that HSA and TQ form a stable complex at physiological pH. CD and FTIR spectroscopic data indicate that the interaction TQ-HSA does not modify the secondary structure of the protein, whilst docking studies and the thermodynamic analysis of the TQ-HSA complex formation indicate that hydrophobic interactions are the predominant forces stabilizing the complex. Finally, displacement experiments and docking studies revealed that TQ binds to site I of HSA. Since HSA, the most abundant protein in blood plasma, regulates the plasmatic concentrations of several drugs, the characterization of the TQ-HSA complex presented in this work covers the lack of information that may be useful for the understanding of TQ pharmacokinetics.

Acknowledgements

Authors are grateful to Italian Ministry of University and Research - Italian-Lebanese International Interuniversity Cooperation - for the support of this research. This work was supported also by a grant from Università Politecnica delle Marche (FT).

References

Arrondo, J.L., Muga, A., Castresana, J., Goni, F.M., 1993. Quantitative studies of the structure of proteins in solution by Fourier-transform infrared spectroscopy. Prog. Biophys. Mol. Biol. 59, 23–56.

Barth, A., Zscherp, C., 2002. What vibrations tell us about proteins. Q. Rev. Biophys. 35, 369–430.

Berman, H.M., Westbrook, J., Feng, Z., Gilliland, G., Bhat, T.N., Weissig, H., Shindyalov, I.N., Bourne, P.E., 2000. The protein data bank. Nucleic Acids Res. 28, 235–242.

Bi, S., Song, D., Kan, Y., Xu, D., Tian, Y., Zhou, X., Zhang, H., 2005. Spectroscopic characterization of effective components anthraquinones in Chinese medicinal herbs binding with serum albumins. Spectrochim. Acta A Mol. Biomol. Spectrosc. 62, 203–212.

Bogdan, M., Pirnau, A., Floare, C., Bugeac, C., 2008. Binding interaction of indomethacin with human serum albumin. J. Pharm. Biomed. Anal. 47, 981–984.

Carter, D.C., Ho, J.X., 1994. Structure of serum albumin. Adv. Protein Chem. 45, 153–203.

Chandra, S., Murthy, S.N., Mondal, D., Agrawal, K.C., 2009. Therapeutic effects of Nigella sativa on chronic HAART-induced hyperinsulinemia in rats. Can. J. Physiol. Pharmacol. 87, 300–309.

Dewar, M.J.S., Zoebisch, E.G., Healy, E.F., Stewart, J.J.P., 1985. Development and use of quantum mechanical molecular models. 76. AM1: a new general purpose quantum mechanical molecular model. J. Am. Chem. Soc. 107, 3902–3909.

Diana, F.J., Veronich, K., Kapoor, A.L., 1989. Binding of nonsteroidal anti-inflammatory agents and their effect on binding of racemic warfarin and its enantiomers to human serum albumin. J. Pharm. Sci. 78, 195–199.

Edris, A.E., 2009. Anti-cancer properties of Nigella spp. essential oils and their major constituents, thymoquinone and beta-elemene. Curr. Clin. Pharmacol. 4, 43–46.

El-Abhar, H.S., Abdallah, D.M., Saleh, S., 2003. Gastroprotective activity of Nigella sativa oil and its constituent, thymoquinone, against gastric mucosal injury induced by ischaemia/reperfusion in rats. J. Ethnopharmacol. 84, 251–258.

El Gazzar, M., El Mezayen, R., Marecki, J.C., Nicolls, M.R., Canastar, A., Dreskin, S.C., 2006. Anti-inflammatory effect of thymoquinone in a mouse model of allergic lung inflammation. Int. Immunopharmacol. 6, 1135–1142.

Gali-Muhtasib, H., Diab-Assaf, M., Boltze, C., Al-Hmaira, J., Hartig, R., Roessner, A., Schneider-Stock, R., 2004a. Thymoquinone extracted from black seed triggers apoptotic cell death in human colorectal cancer cells via a p53-dependent mechanism. Int. J. Oncol. 25, 857–866.

Gali-Muhtasib, H., Roessner, A., Schneider-Stock, R., 2006. Thymoquinone: a promising anti-cancer drug from natural sources. Int. J. Biochem. Cell Biol. 38, 1249–1253.

Gali-Muhtasib, H.U., Abou Kheir, W.G., Kheir, L.A., Darwiche, N., Crooks, P.A., 2004b. Molecular pathway for thymoquinone-induced cell-cycle arrest and apoptosis in neoplastic keratinocytes. Anticancer Drugs 15, 389–399.

Gali-Muhtasib, H., Ocker, M., Kuester, D., Krueger, S., El-Hajj, Z., Diestel, A., Evert, M., El-Najjar, N., Peters, B., Jurjus, A., Roessner, A., Schneider-Stock, R., 2008. Thymoquinone reduces mouse colon tumor cell invasion and inhibits tumor growth in murine colon cancer models. J. Cell Mol. Med. 12, 330–342.

Gelamo, E.L., Silva, C.H., Imasato, H., Tabak, M., 2002. Interaction of bovine (BSA) and human (HSA) serum albumins with ionic surfactants: spectroscopy and modelling. Biochim. Biophys. Acta 1594, 84–99.

Goodsell, D.S., Morris, G.M., Olson, A.J., 1996. Automated docking of flexible ligands: applications of AutoDock. J. Mol. Recognition 9, 1–5.

He, X.M., Carter, D.C., 1992. Atomic structure and chemistry of human serum albumin. Nature 358, 209–215.

Hosseinzadeh, H., Parvardeh, S., Asl, M.N., Sadeghnia, H.R., Ziaee, T., 2007. Effect of thymoquinone and Nigella sativa seeds oil on lipid peroxidation level during global cerebral ischemia-reperfusion injury in rat hippocampus. Phytomedicine 14, 621–627.

Ivankovic, S., Stojkovic, R., Jukic, M., Milos, M., Jurin, M., 2006. The antitumor activity of thymoquinone and thymohydroquinone in vitro and in vivo. Exp. Oncol. 28, 220–224.

Khalife, K.H., Lupidi, G., 2007. Nonenzymatic reduction of thymoquinone in physiological conditions. Free Radical Res. 41, 153–161.

Khan, N., Sultana, S., 2005. Inhibition of two stage renal carcinogenesis, oxidative damage and hyperproliferative response by Nigella sativa. Eur. J. Cancer Prev. 14, 159–168.

Lakowicz, R., 1999. Principles of Fluorescence Spectroscopy. Kluwer Academic/Plenum, New York.

Li, Y., Yao, X., Jin, J., Chen, X., Hu, Z., 2007. Interaction of rhein with human serum albumin investigation by optical spectroscopic technique and modeling studies. Biochim. Biophys. Acta 1774, 51–58.

Loun, B., Hage, D.S., 1994. Chiral separation mechanisms in protein-based HPLC columns. 1. Thermodynamic studies of (R)- and (S)-warfarin binding to immobilized human serum albumin. Anal. Chem. 66, 3814–3822.

Meersman, F., Smeller, L., Heremans, K., 2002. Comparative Fourier transform infrared spectroscopy study of cold-, pressure-, and heat-induced unfolding and aggregation of myoglobin. Biophys. J. 82, 2635–2644.

Mishra, B., Barik, A., Priyadarsini, K.I., Mohan, H., 2005. Fluorescence spectroscopic studies on binding of a flavonoid antioxidant quercetin to serum albumins. J. Chem. Sci. 117, 641–647.

Okuno, A., Kato, M., Taniguchi, Y., 2006. The secondary structure of pressure- and temperature-induced aggregates of equine serum albumin studied by FT-IR spectroscopy. Biochim. Biophys. Acta 1764, 1407–1412.

Padhye, S., Banerjee, S., Ahmad, A., Mohammad, R., Sarkar, F.H., 2008. From here to eternity – the secret of Pharaohs: therapeutic potential of black cumin seeds and beyond. Cancer Ther. 6, 495–510.

Pedretti, A., Villa, L., Vistoli, G., 2002. VEGA: a versatile program to convert, handle and visualize molecular structure on Windows-based PCs. J. Mol. Graph Model 21, 47–49.

Ross, P.D., Subramanian, S., 1981. Thermodynamics of protein association reactions: forces contributing to stability. Biochemistry 20, 3096–3102.

Salomaa, P., Schaleger, L.L., Long, F.A., 1964. Solvent deuterium isotope effects on acid–base equilibria. J. Am. Chem. Soc. 86, 1–7.

Sanner, M.F., 1999. Python: a programming language for software integration and development. J. Mol. Graph Model 17, 57–61.

Shaikh, S.M., Seetharamappa, J., Kandagal, P.B., Manjunatha, D.H., 2007. In vitro study on the binding of anti-coagulant vitamin to bovine serum albumin and the influence of toxic ions and common ions on binding. Int. J. Biol. Macromol. 41, 81–86.

Sudlow, G., Birkett, D.J., Wade, D.N., 1975. The characterization of two specific drug binding sites on human serum albumin. Mol. Pharmacol. 11, 824–832.

Tanfani, F., Galeazzi, T., Curatola, G., Bertoli, E., Ferretti, G., 1997. Reduced beta-strand content in apoprotein B-100 in smaller and denser low-density lipoprotein subclasses as probed by Fourier-transform infrared spectroscopy. Biochem. J. 322 (Pt 3), 765–769.

Timaseff, S.N., 1972. Thermodynamics of protein interactions. In: Peeters, H. (Ed.), Proteins of Biological Fluids. Pergamon Press, Oxford, pp. 511–519.

Whitlam, J.B., Crooks, M.J., Brown, K.F., Pedersen, P.V., 1979. Binding of nonsteroidal anti-inflammatory agents to proteins-I. Ibuprofen-serum albumin interaction. Biochem. Pharmacol. 28, 675–678.

Xie, M.X., Long, M., Liu, Y., Qin, C., Wang, Y.D., 2006. Characterization of the interaction between human serum albumin and morin. Biochim. Biophys. Acta 1760, 1184–1191.

Yi, T., Cho, S.G., Yi, Z., Pang, X., Rodriguez, M., Wang, Y., Sethi, G., Aggarwal, B.B., Liu, M., 2008. Thymoquinone inhibits tumor angiogenesis and tumor growth through suppressing AKT and extracellular signal-regulated kinase signaling pathways. Mol. Cancer Ther. 7, 1789–1796.